sciendo

*Polish Journal of Chemical Technology, 23, **1**, 7—15, 10.2478/pjct-2021-0002*

Synthesis, computational, anticancerous and antiproliferative effects of some copper, manganese and zinc complexes with ligands derived from symmetrical 2,2'-diamino-4,4'-dimethyl-1,1'-biphenyl-salicylaldehyde

Taher S. Ababneh[1*], Mohammad El-Khateeb[2], Aissar K. Tanash[1], Tareq M.A. AL-Shboul[3], Mohammad Jamal A. Shammout[4], Taghreed M.A. Jazzazi[1], Mohammad Alomari[5], Safa Daoud[6], Wamidh H. Talib[7]

[1]*Department of Chemistry, Yarmouk University, Irbid 21163, Jordan*
[2]*Chemistry Department, Jordan University of Science and Technology, Irbid 22110, Jordan*
[3]*Department of Chemistry and Chemical Technology, Tafila Technical University, Tafila, Jordan*
[4]*Department of Basic and Applied Sciences, Zarqa University College, Al-Balqa Applied University, Al-Salt, Jordan*
[5]*Department of Chemistry, University of Petra, Amman 961343, Jordan*
[6]*Department of Pharmaceutical Chemistry and Pharmacognosy, Faculty of Pharmacy, Applied Science Private University, Amman, Jordan*
[7]*Department of Clinical Pharmacy and Therapeutics, Faculty of Pharmacy, Applied Science Private University, Amman, Jordan*
[*]*Corresponding author: e-mail: ababnehtaher@hotmail.com*

Four new symmetrical Schiff bases derived from 2,2'-diamino-4,4'-dimethyl-1,1'-biphenyl-salicylaldehyde have been synthesized and characterized by elemental analysis and different spectroscopic techniques. The reaction of 2,2'-diamino-4,4'-dimethyl-1,1'-biphenyl with two equivalents of 5-tert-butyl-, 3,5-dinitro-, 3,5-dibromo- and 3-tert-butyl-salicylaldehyde yielded 2,2'-bis(5-tert-butyl-salicylideneamino)-4,4'-dimethyl-1,1'-biphenyl (A1) as well as the 3,5-dinitro- (A2), 3,5-dibromo- (A3) and 3-tert-butyl- (A4) substituted derivatives. The tetradentate ligands were then reacted with copper-, manganese- and zinc-acetate producing the tetra-coordinate metal complexes which were characterized by FTIR, UV-Visible spectroscopy, magnetic susceptibility and elemental analysis. Zinc complexes were characterized by 1H-NMR spectroscopy. Density functional theory (DFT) calculations at the B3LYP/6-31G(d) level of theory were carried out to fully optimize and examine the molecular geometries of complexes. Subsequently, IR vibrational and UV-Vis absorption spectra were computed and correlated with the observed values and the results are in good agreement with the experimental data. The anticancerous and antiproliferative activity of the A3 ligand and its metal complexes were determined.

Keywords: Tetradentate Schiff base, Symmetrical metal complexes, DFT calculation, Spectroscopy, Anticancerous, Antiproliferative.

INTRODUCTION

Schiff bases are compounds containing C=NR (R= alkyl, aryl) functional group and are excellent ligands that can coordinate and stabilize metal ions with various oxidation states[1]. They can coordinate to metals through the imine nitrogen and other donor groups, which are usually bound to an aldehyde or a ketone[2].

Schiff bases and their metal complexes have several applications. For instance, Schiff bases are used as catalysts[3], intermediates in organic synthesis[4], polymer stabilizers[5] and in dyes synthesis[6]. On the other hand, Schiff base metal complexes have shown greater biological and pharmaceutical activities compared to the free Schiff base compounds[7–11]. The complexes were found to have a broader application as anti-inflammatory[12], analgesic[13], antimicrobial[14], antitubercular[15], anticancerous[16] and antioxidant[17] agents. Furthermore, Schiff base metal complexes are used as catalysts in many chemical reactions[18–19]. Several Co(II) Schiff base complexes have been used as catalysts in the oxygenation of alkenes[20]. Recently[21–23], the synthesis, characterization and catalytic applications of new metal complexes coordinated with comparable 2,2'-diamino-1,1'-biphenyl-salicylaldehyde Schiff base derivatives have been reported.

Herein, we present the synthesis of new symmetrical tetradentate Schiff bases obtained from the reaction of two equivalents of salicylaldehyde derivatives with 2,2'-diamino-4,4'-dimethyl-1,1'-biphenyl. The copper-, zinc- and manganese-complexes of the resulting Schiff bases were synthesized and characterized. DFT computational studies were conducted to gain a qualitative insight into the structural features and relative energies of the complexes. These calculations revealed detailed vibrational and UV–Vis spectral data of the title complexes and assignments of the computed bands were proposed. Moreover, the anticancerous and antiproliferative activity of the **A3** ligand and its metal complexes were evaluated.

EXPERIMETNAL PART

Materials and methods

The elemental analyses (C, H and N) were carried out on a Perkin Elmer 240 elemental analyzer. ^{1}H- and ^{13}C-NMR spectra were recorded on a Bruker AC 400 spectrometer in $CDCl_3$. Infrared spectra were recorded using KBr on Bruker FT-IR-4100 spectrometer over the range 4000–400 cm^{-1}. Electronic absorption spectra were recorded on PS-2600 Pasco spectrophotometer in DMSO using 8 x 10^{-5} M solutions. Magnetic susceptibility measurements were done using a magnetic susceptibility balance (Johnson Mathey). All commercially available substrates were purchased from Sigma Aldrich or Alfa Aesar and used without further purification. 2,2'-Diamino-4,4'-dimethyl-1,1'-biphenyl was prepared according

to a literature procedure[24]. The entire theoretical modeling of Schiff base complexes was performed using Wavefunction Spartan'18 Parallel Suite on a desktop computer with core i7[25].

General procedure for the preparation of $R(NH_2)_2Me_2$biph (A1-A4)

A mixture of 1.62 mmol of 2,2'-diamino-4,4'-dimethyl--1,1'-biphenyl and 3.24 mmol of salicylaldehyde derivative in absolute ethanol (15 mL) was stirred at reflux for 3 hr. During the reaction, the corresponding Schiff base was precipitated as a stable colored solid. The solid was collected by filtration, washed with cold ethanol and dried under vacuum. All of these ligands are soluble in $CHCl_3$, DMF and DMSO.

*5-tert-Butyl$(NH_2)_2Me_2$biph, **A1*** 0.72 g (83%). Yellow powder. IR (KBr, cm^{-1}): ν_{O-H} 3048 (b); ν_{C-H} 2967 (s); $\nu_{C=N}$ 1621 (s); $\nu_{C=C}$ 1491 (s); ν_{C-O} 1393 (s). ^{1}H-NMR (400 MHz, $CDCl_3$): δ 1.17 (s, 18H, C(CH_3)$_3$), 2.37 (s, 6H, (CH_3), 6.70-7.24 (m, 12H, aromatic-H), 8.44 (s, 2H, N=C*H*), 12.33 (s, 2H, O*H*). ^{13}C NMR (100 MHz, $CDCl_3$): δ 162.8 (N=*C*H), 157.6, 152.5, 145.6, 142.4, 134.9, 132.2, 127.2, 126.8, 124.8, 122.9, 116.8, 115.1 (aromatic-C), 31.7, 30.6 (CMe_3), 21.3 (Me). MS (EI, *m/z*): 533 $[M]^+$. Melting point: 225–228°C. Anal. Calc. for $C_{36}H_{40}N_2O_2$: C, 81.17; H, 7.57; N, 5.26%. Found: C, 80.89; H, 7.66; N, 5.54%.

*3,5-Dinitro$(NH_2)_2Me_2$biph, **A2*** 0.77 g (79%). Orange powder. IR (KBr, cm^{-1}): ν_{O-H} 3068 (b); $\nu_{C=N}$ 1637 (s); $\nu_{C=C}$ 1440 (s)ν_{NO2} 1523 (s), 1482 (s); ν_{C-O} 1337 (s). ^{1}H-NMR (400 MHz, $CDCl_3$): δ 2.50 (s, 6H, (CH_3), 7.46-8.71 (m, 10H, aromatic), 9.46 (s, 2H, N=C*H*), 10.20 (s, 2H, O*H*). ^{13}C NMR (100 MHz, $CDCl_3$): δ 162.1 (N=*C*H), 154.6, 152.3, 143.8, 142.4, 138.9, 130.9, 129.4, 127.6, 126.3, 125.4, 116.9, 115.7 (aromatic-C), 20.8 (Me). MS (EI, *m/z*): 601 $[M]^+$. Melting point: 198–201°C. Anal. Calc. for $C_{28}H_{20}N_6O_{10}$: C; 56.00; H, 3.36; N, 14.00%. Found C; 55.91; H, 3.31; N, 14.06%.

*3,5-Dibromo$(NH_2)_2Me_2$biph, **A3*** 1.01 g (85%). Yellow powder. IR (KBr, cm^{-1}): ν_{O-H} 3068 (b); $\nu_{C=N}$ 1616 (s); $\nu_{C=C}$ 1458 ν_{C-O} 1339 (s); ν_{C-Br} 688 (s). ^{1}H-NMR (400 MHz, $CDCl_3$): δ 2.48 (s, 6H, (CH_3), 6.96-7.69 (m, 10H, aromatic), 8.24 (s, 2H, N=C*H*), 13.42 (s, 2H, O*H*). ^{13}C NMR (100 MHz, $CDCl_3$): δ 162.2 (N=*C*H), 156.7, 156.8, 147.5, 146.1, 135.9, 133.5, 126.8, 125.5, 123.8, 124.3, 116.4, 115.0 (aromatic-C), 21.2 (Me). MS (EI, m/z): 737 $[M]^+$. Melting point: 240–243°C. Anal. Calc. for $C_{28}H_{20}Br_4N_2O_4$: C; 45.69; H, 2.74; N, 3.81%. Found C; 45.59; H, 2.64; N, 3.90%.

*3-tert-Butyl$(NH_2)_2Me_2$biph, **A4*** 1.01 g (85%). Yellow powder. IR (KBr, cm^{-1}): ν_{O-H} 3060 (b); ν_{C-H} 2951 (s); $\nu_{C=N}$ 1630 (s); $\nu_{C=C}$ 1425; ν_{C-O} 1376 (s). ^{1}H-NMR (400 MHz, $CDCl_3$): δ 1.27 (s, 18H, C(CH_3)$_3$), 2.36 (s, 6H, (CH_3), 6.56-7.23 (m, 12H, aromatic-H), 8.25 (s, 2H, N=C*H*), 13.24 (s, 2H, O*H*). ^{13}C NMR (100 MHz, $CDCl_3$): δ 164.9 (N=*C*H), 155.9, 150.5, 144.2, 142.3, 138.5, 131.7, 129.8, 128.4, 126.2, 123.8, 118.4, 116.5 (aromatic-C), 34.2, 33.7 (CMe_3), 21.2 (Me). MS (EI, m/z): 533 $[M]^+$. Melting point: 226–228°C. Anal. Calc. for $C_{36}H_{40}N_2O_2$: C; 80.92; H, 7.57; N, 5.26%. Found C; 80.92; H, 7.56; N, 5.38%.

General Procedure for the Preparation of Complexes (CuA1-CuA4), (MnA1-MnA4), (ZnA1-ZnA4)

To a stirred solution of 1.62 mmol Schiff base in 20 mL ethanol, 1.62 mmol of copper(II) acetate monohydrate, manganese(II) acetate tetrahydrate or zinc(II) acetate dihydrate was added at room temperature. The reaction mixture was heated for 6 hrs at 60°C. During the reaction, the corresponding complex was precipitated as a colored solid which was precipitated, filtered, washed with cold ethanol and dried as a stable colored powder. All of these complexes are soluble in $CHCl_3$ and DMSO.

*Cu(II)[5-tert-Butyl$(NH_2)_2Me_2$biph], **CuA1*** 0.79 g (76%). Green powder. IR (KBr, cm^{-1}): ν_{C-H} 2967 (s); $\nu_{C=N}$ 1606 (s); $\nu_{C=C}$ 1590 (s); ν_{C-O} 1385 (s); ν_{M-O} 590 (m); ν_{M-N} 450 (w). MS (EI, m/z): 595 $[M]^+$. Melting point: 245–248°C. Anal. Calc. for $CuC_{36}H_{38}N_2O_2$: C; 72.76; H, 6.45; N, 4.71%. Found C; 71.98; H, 6.85; N, 4.59%.

*Cu(II)[3,5-Dinitro$(NH_2)_2Me_2$biph], **CuA2*** 0.83 g (77%). Green powder. IR (KBr, cm^{-1}): $\nu_{C=N}$ 1614 (s); $\nu_{C=C}$ 1467 (s); ν_{NO2} 1530, 1472 (s); ν_{C-O} 1327 (s); ν_{M-O} 533 (m); ν_{M-N} 443 (w). MS (EI, m/z): 663 $[M]^+$. Melting point: 295–298°C. Anal. Calc. for $CuC_{28}H_{18}N_6O_{10}$: C; 50.80; H, 2.74; N, 12.69%. Found C; 50.65; H, 2.57; N, 12.78%.

*Cu(II)[3,5-Dibromo$(NH_2)_2Me_2$biph], **CuA3*** 0.94 g (73%). Green powder. IR (KBr, cm^{-1}): $\nu_{C=N}$ 1582 (s); $\nu_{C=C}$ 1508 (s); ν_{C-O} 1303 (s); ν_{C-Br} 698 (s); ν_{M-O} 533 (s); ν_{M-N} 442 (w). MS (EI, m/z): 798 $[M]^+$. Melting point: 284–287°C. Anal. Calc. for $CuC_{28}H_{18}N_2O_2Br_4$: C; 42.16; H, 2.27; N, 3.51%. Found C; 42.01; H, 2.13; N, 3.49%.

*Cu(II)[3-tert-Butyl$(NH_2)_2Me_2$biph], **CuA4*** 0.77 g (74%). Green powder. IR (KBr, cm^{-1}): ν_{C-H} 2958 (s); $\nu_{C=N}$ 1606 (s); $\nu_{C=C}$ 1418 (s); ν_{C-O} 1319 (s); ν_{M-O} 516 (s); ν_{M-N} 426 (w). MS (EI, m/z): 596 $[M]^+$. Melting point: 242–245°C. Anal. Calc. for $CuC_{36}H_{38}N_2O_2$: C; 72.76; H, 6.82; N, 4.71%. Found C; 71.97; H, 6.82; N, 4.49%.

*Mn(II)[5-tert-Butyl$(NH_2)_2Me_2$biph], **MnA1*** 0.74 g (78%). Bright yellow powder. IR (KBr, cm^{-1}): ν_{C-H} 2951 (s); $\nu_{C=N}$ 1606 (s); $\nu_{C=C}$ 1484 (s); ν_{C-O} 1360 (s); ν_{M-O} 533 (m); ν_{M-N} 405 (w). MS (EI, m/z): 586 $[M]^+$. Melting point: 223–226°C. Anal. Calc. for $MnC_{36}H_{38}N_2O_2$: C; 73.83; H, 6.54; N, 4.78%. Found C; 73.77; H, 6.51; N, 4.63%.

*Mn(II)[3,5-Dinitro$(NH_2)_2Me_2$biph], **MnA2*** 0.77 g (73%). Bright yellow powder. IR (KBr, cm^{-1}): $\nu_{C=N}$ 1614 (s); ν_{NO2} 1556, 1517 (s); $\nu_{C=C}$ 1467 (s); ν_{C-O} 1327 (s); ν_{M-O} 533 (m); ν_{M-N} 443 (w). MS (EI, m/z): 654 $[M]^+$. Melting point: 297–300°C. Anal. Calc. for $MnC_{28}H_{18}N_6O_{10}$: C; 51.47; H, 2.78; N, 12.68%. Found C; 50.77; H, 2.59; N, 12.75%.

*Mn(II)[3,5-Dibromo$(NH_2)_2Me_2$biph], **MnA3*** 0.91 g (72%). Bright yellow powder. IR (KBr, cm^{-1}): $\nu_{C=N}$ 1598 (s); $\nu_{C=C}$ 1458 (s); ν_{C-O} 1303 (s); ν_{C-Br} 672 (s); ν_{M-O} 533 (s); ν_{M-N} 442 (w). MS (EI, m/z): 790 $[M]^+$. Melting point: 285–288°C. Anal. Calc. for $MnC_{28}H_{18}N_2O_2Br_4$: C; 42.62; H, 2.30; N, 3.55%. Found C; 41.94; H, 2.24; N, 3.43%.

*Mn(II)[3-tert-Butyl$(NH_2)_2Me_2$biph], **MnA4*** 0.70 g (74%). Bright yellow powder. IR (KBr, cm^{-1}): ν_{C-H} 2958 (s); $\nu_{C=N}$ 1606 (s); $\nu_{C=C}$ 1426 (s); ν_{C-O} 1319 (s); ν_{M-O} 533 (s); ν_{M-N} 410 (w). MS (EI, m/z): 586 $[M]^+$. Melting point: 220–223°C. Anal. Calc. for $MnC_{36}H_{38}N_2O_2$: C; 73.83; H, 6.44; N, 4.73%. Found C; 73.27; H, 6.44; N, 4.73%.

*Zn(II)[5-tert-Butyl$(NH_2)_2Me_2$biph], **ZnA1*** 0.78 g (81%). Yellow powder. IR (KBr, cm^{-1}): ν_{C-H} 2972 (s); $\nu_{C=N}$ 1612 (s); $\nu_{C=C}$ 1491 (s); ν_{C-O} 1361 (s); ν_{M-O} 616 (m);

ν_{M-N} 479 (w). ^{1}H-NMR (400 MHz, $CDCl_3$): δ 1.16 (s, 18H, C(CH_3)$_3$), 2.38 (s, 6H, (CH_3)), 6.72-7.25 (m, 12H, aromatic), 8.46 (s, 2H, N=C*H*). ^{13}C NMR (100 MHz, $CDCl_3$): δ 168.3 (N=*C*H), 166.5 (CO), 146.8, 140.7, 135.7, 133.7, 130.8, 129.3, 128.9, 125.6, 123.2, 121.1, 116.0 (aromatic-C), 30.0, 23.9 (CMe_3), 20.1 (Me). MS (EI, m/z): 597 $[M]^+$. Melting point: 224–227°C. Anal. Calc. for $ZnC_{36}H_{38}N_2O_2$: C; 72.54; H, 6.43; N, 4.70%. Found C; 72.33; H, 6.42; N, 4.64%.

Zn(II)[3,5-Dinitro(NH$_2$)$_2$Me$_2$biph], ***ZnA2*** 0.87 g (81%). Yellow powder. IR (KBr, cm^{-1}): $\nu_{C=N}$ 1621 (s); ν_{NO2} 1556, 1527 (s); $\nu_{C=C}$ 1421 (s); ν_{C-O} 1337 (s); ν_{M-O} 544 (m); ν_{M-N} 483 (w). ^{1}H-NMR (400 MHz, $CDCl_3$): δ 2.34 (s, 6H, (CH_3), 6.94–8.63 (m, 10H, aromatic), 8.64 (s, 2H, N=C*H*). ^{13}C NMR (100 MHz, $CDCl_3$): δ 167.1 (N=*C*H), 165.8 (CO), 145.6, 141.7, 134.9, 132.7, 132.2, 126.8, 125.3, 121.0, 119.6, 118.1, 116.3 (aromatic-C), 20.2 (Me). MS (EI, m/z): 664 $[M]^+$. Melting point: 300–303°C. Anal. Calc. for $ZnC_{28}H_{18}N_6O_{10}$: C; 50.66; H, 2.73; N, 12.66%. Found C; 50.41; H, 2.51; N, 12.54%.

Zn(II)[3,5-Dibromo(NH$_2$)$_2$Me$_2$biph], ***ZnA3*** 1.04 g (80%). Yellow powder. IR (KBr, cm^{-1}): $\nu_{C=N}$ 1604 (s); $\nu_{C=C}$ 1499 (s); ν_{C-O} 1377 (s); ν_{C-Br} 682 (s); ν_{M-O} 544 (s); ν_{M-N} 438 (w). ^{1}H-NMR (400 MHz, $CDCl_3$): δ 2.33 (s, 6H, (CH_3), 6.82–7.68 (m, 10H, aromatic), 8.04 (s, 2H, N=C*H*). ^{13}C NMR (100 MHz, $CDCl_3$): δ 168.1 (N=*C*H), 163.6 (CO), 145.9, 141.3, 139.4, 135.0, 131.5, 127.8, 124.9, 123.2, 120.5, 117.7, 115.6 (aromatic-C), 20.9 (Me). MS (EI, m/z): 800 $[M]^+$. Melting point: 282–285°C. Anal. Calc. for $ZnC_{28}H_{18}N_2O_2Br_4$: C; 42.07; H, 2.27; N, 3.50%. Found C; 42.13; H, 2.26; N, 3.41%.

Zn(II)[3-tert-Butyl(NH$_2$)$_2$Me$_2$biph], ***ZnA4*** 0.71 g (73%). Yellow powder. IR (KBr, cm^{-1}): ν_{C-H} 2968 (s); $\nu_{C=N}$ 1610 (s); $\nu_{C=C}$ 1490 (s); ν_{C-O} 1357 (s); ν_{M-O} 612 (s); ν_{M-N} 465 (w). ^{1}H-NMR (400 MHz, $CDCl_3$): δ 1.26 (s, 18H, C(CH_3)$_3$), 2.47 (s, 6H, (CH_3), 6.89–7.50 (m, 12H, aromatic), 8.56 (s, 2H, N=C*H*). ^{13}C NMR (100 MHz, $CDCl_3$): δ 170.8 (N=*C*H), 168.8 (CO), 147.8, 142.1, 140.1, 136.0, 132.3, 131.1, 130.4, 129.7, 127.1, 121.5, 117.1 (aromatic-C), 31.1, 25.6 (CMe_3), and 20.6 (Me). MS (EI, m/z): 586 $[M]^+$. Melting point: 223–227°C. Anal. Calc. for $ZnC_{36}H_{38}N_2O_2$: C; 74.54; H, 6.43; N, 4.70%. Found C; 72.48; H, 6.38; N, 4.57%.

Computational Method

Schiff base complexes were fully optimized in the gas phase at the B3LYP/6-31G(d) level of theory[26–30] without any geometry or symmetry constraints. The absence of imaginary frequencies in the vibrational analysis was taken as evidence that the optimized complexes represent stable minimal-energy geometries.

Antiproliferative Assay

The antiproliferative effect of **A3** ligand and its three metal complexes was determined using 3-(4,5-dimethylthiazol2-yl)-2,5-diphenyltetrazolium bromide(MTT) assay. This assay measures the reduction of MTT by mitochondrial dehydrogenase (of viable cells) to blue formazan product, which reflects the normal function of mitochondria and cell viability. The procedure was performed as previously described[31]. Briefly, MCF-7 (human breast carcinoma cell line), HCT 116 (human colon cancer cell line) as well as Vero (monkey kidney) normal cell lines were cultured in flat bottom 96-well microplates (1.5×10^4 cells per well) in a complete tissue culture medium supplemented with 10% fetal bovine serum (FBS), 1% L-glutamine, 1% penicillin-streptomycin, and 0.1% gentamycin. These cell lines were selected to test the ability of compounds to target cancers arising from different tissues. Cells were incubated overnight at 37°C in a 5% CO_2 enriched atmosphere. Then cells were exposed to increasing concentrations of the ligand or its three metal complexes (50–320 μM). After 48 hours of incubation with different compounds, MTT dye was added to the wells according to the instructions in the kit (Sigma-Aldrich, Missouri, USA). After 4 hr incubation with the MTT solution, blue crystals were produced. The reaction was terminated by adding 100 µl of the stop solution for 1 hr. Reduced MTT (dark blue color) was assayed using microplate reader (Biotek, Winooski, VT, USA) at a wavelength of 550 nm. The percentage of survival was calculated using the following equation:

% Survival = treated cells absorbance/negative control absorbance × 100%

The calculated inhibitory concentration (IC_{50}) represents the treatment concentration that showed a lethal effect on 50% of cells. Cells treated with cisplatin were used as a positive control and those incubated with culture medium alone were used as a negative control.

RESULTS AND DISCUSSION

Synthesis

New symmetrical Schiff bases 2,2'-diamino-4,4'-dimethyl-1,1'-biphenyl-salicylaldehyde (**A1, A2, A3,** and **A4**) were prepared *via* the reaction of 2,2'-diamino-4,4'-dimethyl-1,1'-biphenyl with two equivalents of salicylaldehyde derivative: 5-*tert*-butyl-, 3,5-dinitro-, 3,5-dibromo-, or 3-*tert*-butyl-salicylaldehyde to produce the desired tetradentate Schiff base ligands, as shown in Scheme 1.

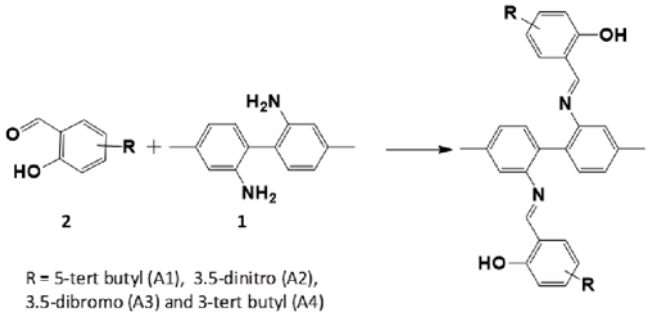

Scheme 1. Synthesis of 2,2'-diamino-4,4'-dimethyl-1,1'-biphenyl--salicylaldehyde Schiff base ligands (**A1-A4**)

The corresponding copper (**CuA1-CuA4**), manganese (**MnA1-MnA4**) and zinc (**ZnA1-ZnA4**) complexes were prepared by the reaction of copper-, manganese- or zinc-acetate with the corresponding ligands **A1–A4** in absolute ethanol as shown in Scheme 2.

Substitution of nitro, bromo, or *tert*-butyl on the aromatic ring of the salicylaldehyde precursor does not prevent the condensation reaction of 2,2'-diamino-4,4'-dimethyl-1,1'-biphenyl with various aldehydes and the corresponding Schiff bases **A1–A4** were effectively synthesized with approximately similar yields.

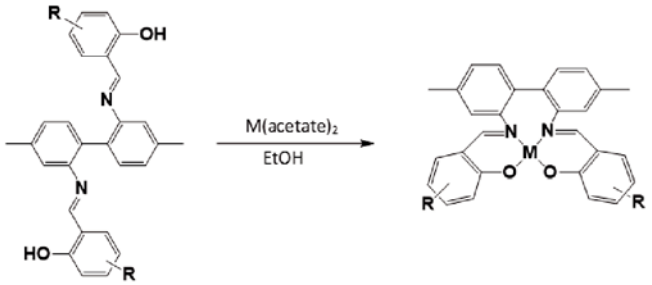

Scheme 2. Synthesis of 2,2'-diamino-4,4'-dimethyl-1,1'-biphenyl-salicylaldehyde metal complexes (**CuA1-CuA4**), (**MnA1-MnA4**) and (**ZnA1-ZnA4**)

Infrared spectroscopy

Infrared spectra of the prepared copper, manganese and zinc complexes exhibit a shift in the characteristic peak of the imine (-C=N-) moiety compared to that of the free ligands, as shown in Table 1.

Table 1. Selected infrared bands of Schiff base ligands and their complexes

ν(C = N) (cm^{-1})	1	2	3	4
A	1621	1637	1616	1630
CuA	1606	1614	1582	1606
MnA	1606	1614	1598	1606
ZnA	1612	1621	1604	1610

A shift in the position of ν(C=N) is usually an indication of the involvement of this group in the metal coordination[21]. The observed ν(C=N) frequency of the metal complexes is shifted to a lower value indicating complexation from the two azomethine nitrogen atoms.

The broad bands observed in the free ligands (**A1-A4**) spectra at 3048, 3068, 3065 and 3060 cm^{-1}, respectively, and attributed to the OH group, disappeared in the case of complexes due to deprotonation and verifying that the Schiff base ligands are also coordinated to the metal ions via phenolic oxygen atoms resulting in a (ONNO)-tetradentate coordination to the metal ions. The normal free O-H stretching frequency ranges from 3500–3600 cm^{-1}. However, due to strong intermolecular hydrogen bonding between enolic O-H and the nitrogen of the azomethine group (O-H----N) the frequencies are reduced to 3048–3060 cm^{-1}.

The weak bands in the lower wavelength regions 401–483 cm^{-1} (avg. 444 cm^{-1}) and 511–616 cm^{-1} (avg. 538 cm^{-1}) are assigned to the stretching frequencies of M–N and M-O bands, respectively, for the metal complexes suggesting the complexation through nitrogen and oxygen atoms from the ligand[32–33].

UV-Visible spectroscopy

The UV-Vis electronic spectra of the ligands **A1-A4** and complexes in DMSO using 8 x 10^{-5} M solutions are given in Table 2. Stemming from the conjugated nature of prepared Schiff base ligands, two absorption bands

Table 2. Electronic absorption data of the Schiff base complexes measured at room temperature in DMSO using 8 x 10^{-5} M solutions

Compound	Absorption (nm)	$\varepsilon \times 10^3$ ($M^{-1}\cdot cm^{-1}$)
A1	275, 354	12.58, 10.33
A2	303, 385	12.38, 28.46
A3	270, 358	25.08, 19.26
A4	274, 352	24.66, 20.42
MnA1	275, 388	26.00, 20.70
MnA2	255, 390	50.00, 28.45
MnA3	257, 389	25.41, 18.96
MnA4	255, 389	39.41, 13.01
CuA1	274, 411	13.28, 5.31
CuA2	261, 390	48.17, 38.77
CuA3	275, 390	48.25, 46.87
CuA4	257, 411	23.15, 7.69
ZnA1	284, 388	47.62, 24.71
ZnA2	260, 392	42.24, 39.30
ZnA3	260, 393	32.79, 14.24
ZnA4	283, 390	21.86, 12.25

below 450 nm appeared and were attributed to intra-ligand charge-transfer absorptions; $\pi\rightarrow\pi^*$ and $n\rightarrow\pi^*$, of the conjugated system and the azomethine group, respectively[34]. These bands also exist in the spectra of all complexes but undergo shifts in absorption peaks especially apparent in the lower-energy band (red shift) of the $n\rightarrow\pi^*$ transition. This shift in the spectra of the synthesized complexes supports the coordination of the ligand to metal ions (Fig. 1). Usually, d-d transitions are not easily detected since they may be obscured by the broad charge transfer (CT) transition tailing off into the visible spectra[35].

NMR spectroscopy

NMR spectroscopy is utilized to characterize the zinc complexes, whereas copper and manganese complexes were inactive in this spectroscopic technique. The ^{1}H-NMR spectra of zinc complexes show an absence of OH proton peaks, which appear at 12.33, 10.20, 13.42 and 13.24 ppm in the free ligands (**A1-A4**), respectively. This indicates loss of protons from the two hydroxyl groups in the free ligand and possible formation of new bonds between the metal and the two oxygen atoms. Another spectroscopic evidence for the formation of these complexes comes from ^{1}H-NMR in which characteristic peaks of (-CH=N-) proton, which appears at 8.46, 8.64, 8.04 and 8.56 ppm for **(ZnA1-ZnA4),** respectively, is shifted from 8.44, 9.46, 8.24 and 8.25 ppm in the free ligands **(A1-A4),** respectively. These ^{1}H-NMR values for both the free ligands and zinc complexes are compatible with those reported for similar compounds such as 2,2'-bis(2-oxidobenzylideneamino)-4,4'-dimethyl-dibromo-1,1'-biphenyl derivatives and their corresponding zinc complexes[22].

Magnetic susceptibility measurements

The magnetic susceptibility measurements reveal an average effective magnetic moment value for the copper complexes of 1.81 B.M., manganese complexes of 5.93 B.M. and zinc complexes of ~0 B.M. These values are expected for the dipositive zinc and copper ions in which Zn(II) with $3d^{10}$ configuration is diamagnetic and Cu(II) is paramagnetic with one unpaired electron ($3d^9$). For Mn(II) $3d^5$ configuration, with two possibilities; high-spin

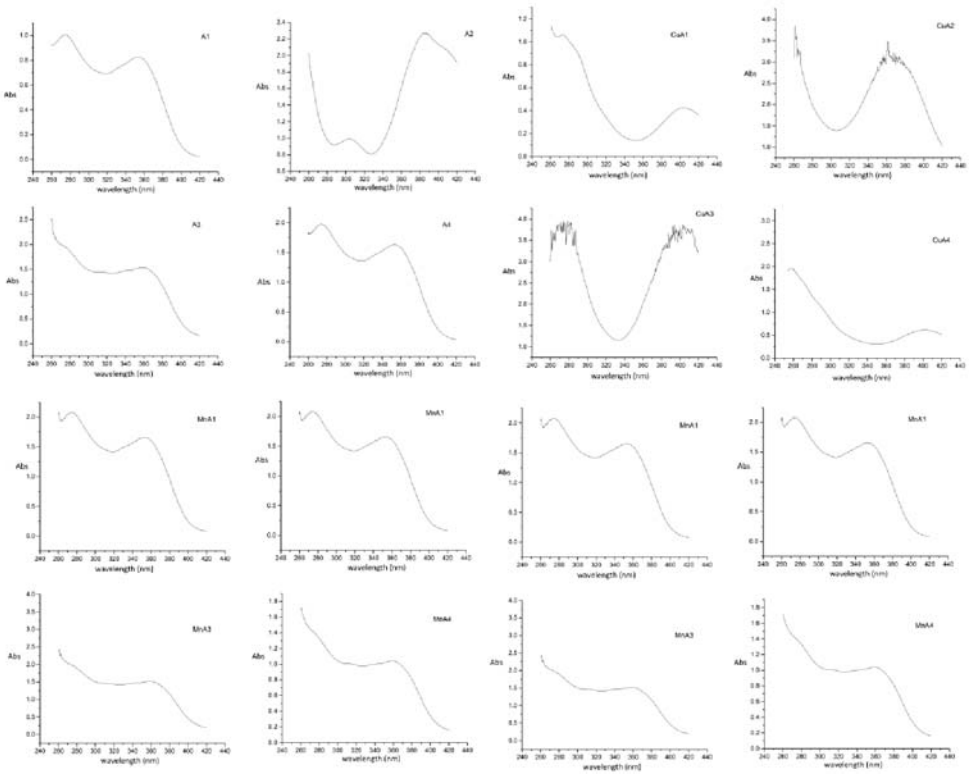

Figure 1. UV-VIS absorption spectra of A1-A4 ligands and their metal complexes at room temperature in 8 x 10^{-5} M DMSO solutions

(5 unpaired e^-) and low-spin (1 unpaired e^-) arrangements, the detected magnetic moment of 5.93 B.M., will leave no doubt that the five d-electrons of Mn(II) are distributed in a high-spin arrangement, which implies that the Mn(II) complexes would have a tetrahedral--based geometry.

Computational study

DFT calculations were carried out to investigate the structure, energy and properties of the title neutral monoligated Cu, Zn and Mn complexes at the B3LYP/6––31G(d) level of theory. Selected structural parameters of the optimized complexes are listed in Table 3, where bond lengths are in Å and angles are in degrees.

Table 3. Selected calculated bond lengths (Å) and angles (°) of the complexes

	CuA1	ZnA1	MnA1	CuA2	ZnA2	MnA2
Bond (Å)						
M-O1	1.897	1.919	1.978	1.902	1.924	1.983
M-O2	1.900	1.921	1.981	1.901	1.924	1.983
M-N1	1.958	2.005	2.139	1.948	1.995	2.135
M-N2	1.952	2.006	2.139	1.947	1.998	2.136
C1=N1	1.309	1.305	1.305	1.301	1.298	1.298
C2=N2	1.310	1.307	1.307	1.301	1.298	1.298
Angle (°)						
O1-M-O2	93.68	111.43	120.19	93.79	111.11	121.13
O1-M-N1	94.79	95.65	89.18	94.35	94.83	87.75
N1-M-N2	98.67	98.35	94.58	99.70	100.39	95.87
N2-M-O2	94.79	95.45	89.17	94.45	94.67	87.79
O1-M-N2	144.21	129.66	134.17	143.34	129.83	134.62
O2-M-N1	143.59	129.91	133.19	143.78	129.95	133.83
	CuA3	**ZnA3**	**MnA3**	**CuA4**	**ZnA4**	**MnA4**
Bond (Å)						
M-O1	1.902	1.921	1.982	1.904	1.921	1.978
M-O2	1.900	1.924	1.981	1.897	1.916	1.972
M-N1	1.949	2.001	2.138	1.943	1.994	2.127
M-N2	1.951	2.002	2.139	1.944	1.998	2.130
C1=N1	1.305	1.302	1.302	1.308	1.306	1.306
C2=N2	1.305	1.302	1.302	1.308	1.306	1.306
Angle (°)						
O1-M-O2	94.50	112.68	122.37	95.10	111.07	120.76
O1-M-N1	94.29	94.93	88.22	94.13	94.79	88.25
N1-M-N2	99.14	99.38	95.12	99.47	99.17	95.04
N2-M-O2	94.51	94.77	88.14	94.29	94.36	87.96
O1-M-N2	143.16	129.16	133.50	142.60	130.64	134.75
O2-M-N1	143.82	129.33	132.53	143.47	131.05	134.21

The optimized geometries of the copper complexes are depicted in Figures 2 and 3. These Figures also elucidate the molecular structures of the Zn and Mn complexes since our data suggest an analogous coordination environment around the metal ions. The results from the geometrical optimization of the complexes show that the complexes exhibit the same tetradentate coordination around the metal ion with a distorted geometry.

The M(II) center (M=Cu, Mn, Zn) is in an intermediate coordination sphere between tetrahedral and planar arrangement of the donor atoms with an average angle between the O1-M-O2 and N1-M-N2 planes of 49.3°, 56.1 and 64.2° whereas the average angle between the O1-M-N1 and O2-M-N2 planes is 50.1°, 64.5° and 69.5° for the Cu, Mn and Zn complexes, respectively. This trend is closely attuned to the increase in atomic size across this series of metals.

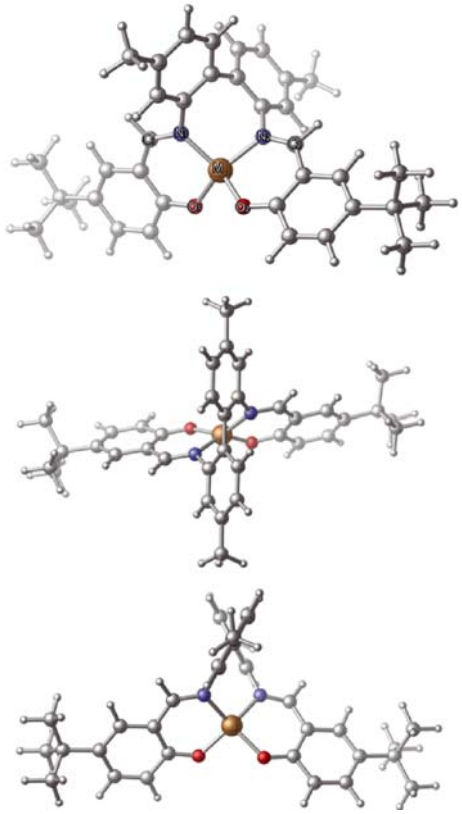

Figure 2. Different views of the optimized ground-state geometry for the copper(II) complex with **A1** ligand at the B3LYP/6-31G(d) level of theory showing the atom-numbering scheme around the metal ion

The calculated C–C bond length between aryl units of the biphenyl backbone across all twelve complexes exhibits a typical single bond value averaging 1.494 Å, thus ruling out interactions between π-systems of these moieties. This result is close to the reported value of 1.491 Å for a comparable zinc complex[22] for which the biphenyl backbone is twisted with an angle of 56.5° between the aryl planes, which is also comparable to an average value of 58.67° calculated for **ZnAn** (n = 1,2,3) complexes. The relatively larger torsion angles in these ligands could be attributed to the lack of bulky groups at the biphenyl backbone allowing for some flexibility in such systems.

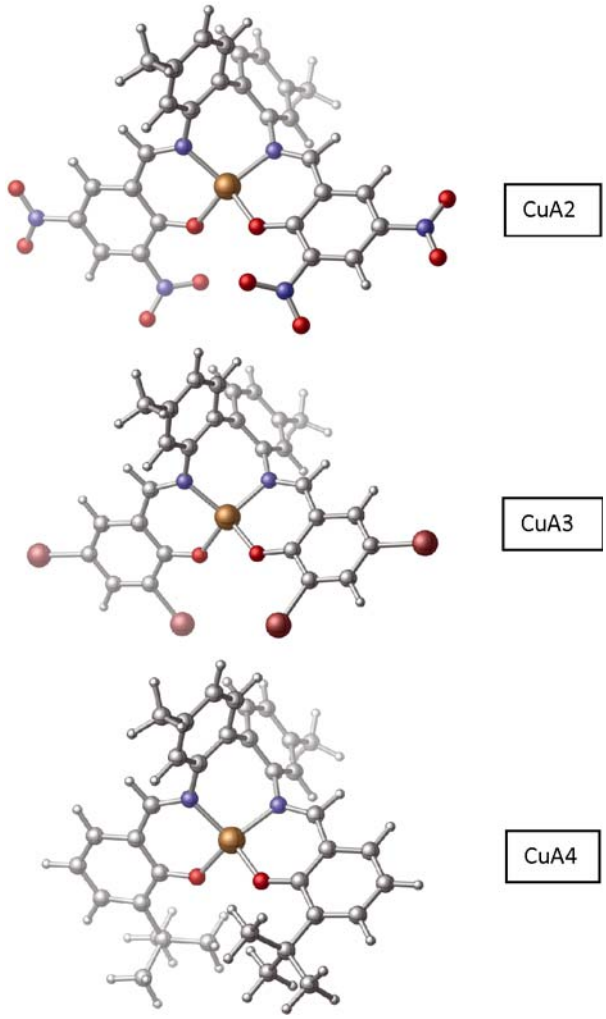

Figure 3. Perspective views of the optimized ground-state geometries for the **A2**, **A3** and **A4** copper complexes at the B3LYP/6-31G(d) level of theory

In all complexes, the calculated M-O bond distance ranges from 1.897–1.983 Å with an average length of 1.934 Å, while the computed M-N bond distance ranges from 1.943–2.139 Å (average of 2.028 Å). These variations in bond distances are only considered when going from a group of all-copper complexes to another of all-zinc complexes, etc. However, by only taking into account complexes of one metal ion as a group (e.g. CuA1, CuA2, etc.), we can see that such variations in bond distances are minute. For example, average Cu-O bond distances in going from CuA1 to CuA4 is 1.898, 1.901, 1.900 and 1.900 Å, respectively. This similarity reflects the fact that the coordination environment around the metal ion in the complexes is not directly influenced by the type of substituent on the ligand, but rather by the type of metal ion and its unique electronic configuration. The calculated Cu-O and Cu-N average bond distances in all investigated copper complexes are 1.900 and 1.949 Å, respectively. This result is in good agreement with a similar XRD-resolved copper complex reported recently in our lab[36] in which the experimental Cu-O and Cu-N average bond distances are 1.903 and 1.958 Å, respectively.

The bond angles of neighboring sites in the MN_2O_2 core follow a similar pattern. For example, the average O1-M-O2 angle is calculated at 94.24° for the Cu complexes, 111.57° for the Zn complexes and 121.11°

for the Mn complexes. The geometry generally is based on an arrangement of electron pairs. Since Mn(II) complexes have five unpaired electrons, their d-orbitals are only half filled, thus it demands less space, and the O-M-O angle opens up a little to 121.11° (on average). The calculated bond angles of O1-Cu-O2 (94.24°) and N1-Cu-N2 (99.24°) are considerably similar to the values found in the literature for unsubstituted copper(II) 2,2'-(2-oxidobenzylideneamino)-1,1'-biphenyl (89°–96°)[37].

Other factors that have a significant role in determining the geometry around the metal are steric constraints imposed by the multidentate ligands. These are of particular importance in our case since such large ligands (**A1** to **A4**) force the complex into a distorted geometry so the ligand can be less restraint and confined.

In addition to the ground-state geometrical optimization, calculations on several low-lying excited states (100 states were used) were carried out to produce a UV/visible spectrum. Calculations performed at the B3LYP/6-31G(d) level of theory on the **CuA1** complex resulted in an electronic absorption spectrum with λ_{max} of 312 and 395 nm. This result is in good agreement with the experimental λ_{max} of 274 and 411 nm (Fig. 4).

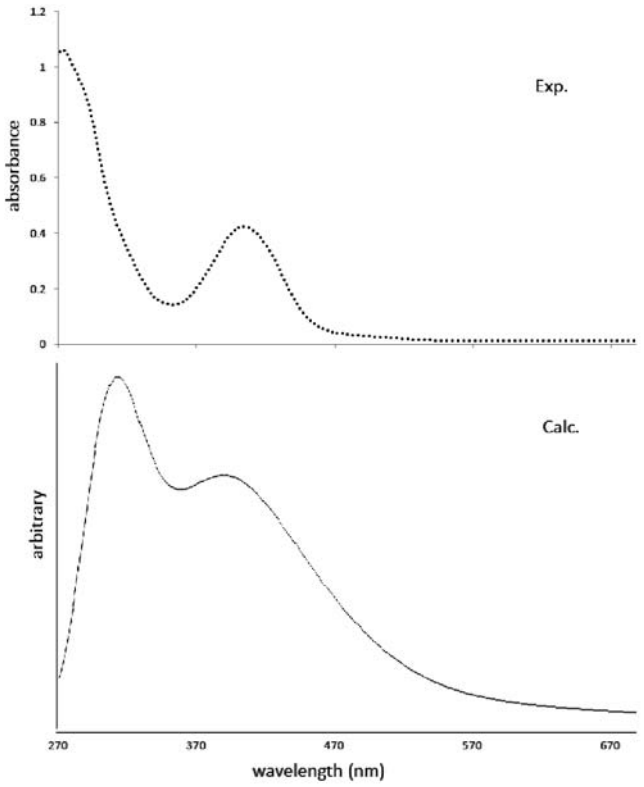

Figure 4. Comparison of DFT-calculated and experimental absorption spectra for the **A1**-copper complex. λ_{max}: computed = 312, 395 nm, experimental = 274, 411 nm

The vibrational analysis was also conducted in which the IR vibrational wavenumbers were computed and compared with the experimentally determined values. The computed FT-IR vibrational analysis of the ligands (Fig. 5) reveals a strong band at 1608–1610 cm^{-1} assigned to the C=N stretching of the ligands and in good agreement with the experimentally determined IR spectra. Another calculated absorption band at 1561–1577 cm^{-1} is assigned to the C=C stretching mode. The broad band observed in the 3048–3068 cm^{-1} region in the IR spectrum

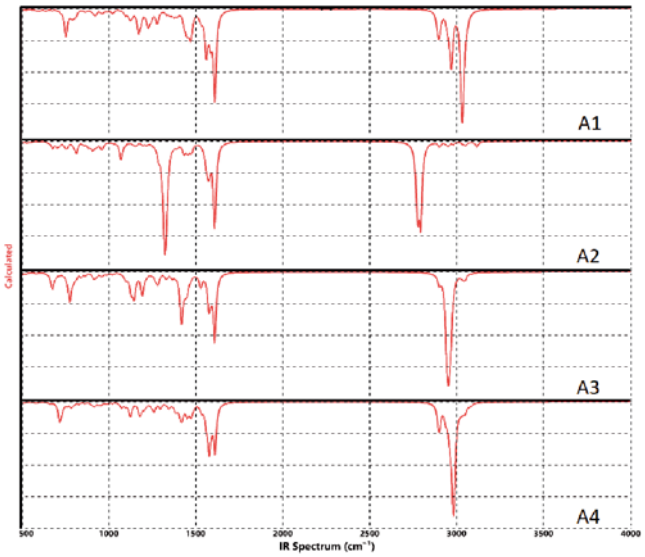

Figure 5. Calculated IR spectra for **A1**, **A2**, **A3** and **A4** ligands

and associated with the O-H stretching vibrations ν(O-H) is theoretically predicted at 2800–3035 cm^{-1}. Strong characteristic peaks appear in the IR spectrum **A2** ligand at 1320 and 1562 cm^{-1} are attributed to ν(NO_2) stretching modes[38]. The absorption band associated with ν(C-Br) in **A3** is calculated at 678 cm^{-1} and in good agreement with the experimentally determined peak at 688 cm^{-1}.

For comparison reasons in regards to the complexes, two sets of IR spectra were computed and grouped. The first is IR spectra of **CuA1**, **CuA2**, **CuA3** and **CuA4** (Fig. 6), while the second set consists of IR spectra of **CuA1**, **ZnA1** and **MnA1**, which have very similar spectral fingerprint (Fig. 7).

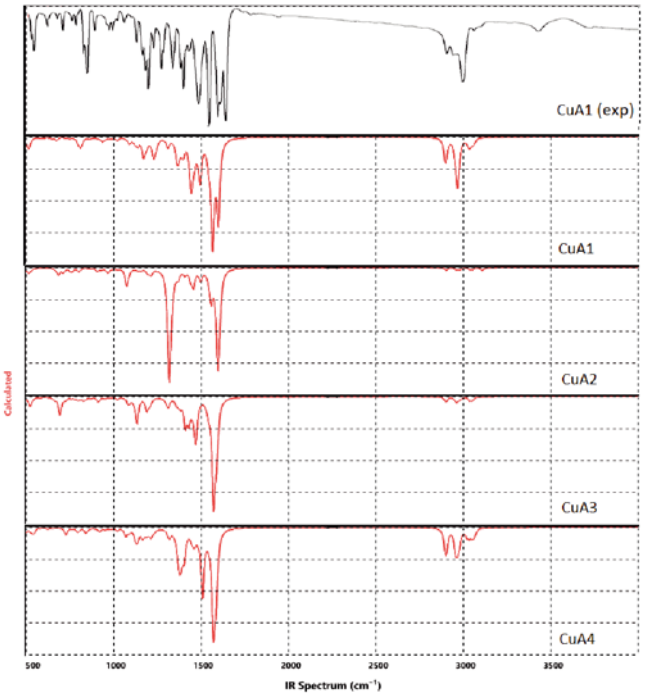

Figure 6. Calculated IR spectra for **CuA1**, **CuA2**, **CuA3** and **CuA4** complexes. Experimental CuA1 IR spectrum is shown (top) for reference

Comparing the computed IR spectrum of **CuA1** complex with the experiment (Fig. 7, top), we find the presence of an absorption band attributable to ν(C=N) at 1570 cm^{-1} (exp. 1606 cm^{-1}), a wide absorption band in

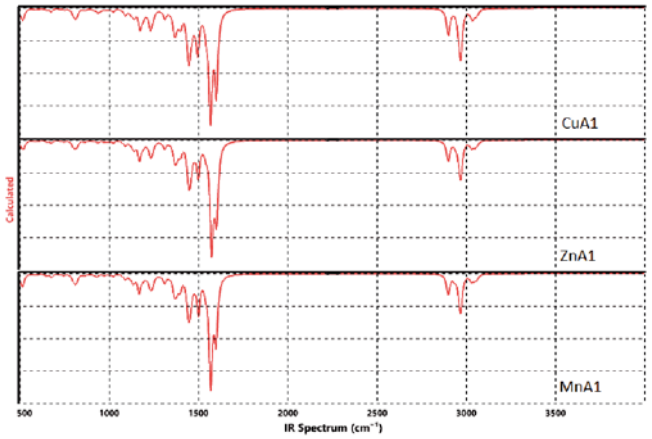

Figure 7. Calculated IR spectra for **CuA1**, **ZnA1** and **MnA1** complexes

the range of 2894–3064 cm^{-1} (exp. 2951 cm^{-1}) attributed to the υ(C-H), an absorption band in the range of 1496-1543 cm^{-1} (exp. 1484 cm^{-1}) assigned to υ(C=C), a band at 1392 cm^{-1} (exp. 1360 cm^{-1}) assigned to the υ(C-O) and a band at 519 cm^{-1} (exp. 533 cm^{-1}) attributed to the υ(Cu-O). In the computed IR spectrum of **CuA2** complex, two characteristic bands appear at 1319 and 1559 cm^{-1} (exp. 1351 and 1530 cm^{-1}) which are attributed to the NO_2 vibrational modes. A distinctive peak at 692 cm^{-1} (exp. 698 cm^{-1}) appears in the IR spectrum of **CuA3** is attributable to υ(C-Br). The spectrum of **CuA4** complex shows a strong absorption band at 1569 cm^{-1} (exp. 1606 cm^{-1}) assigned to υ(C=N) while υ(C=C) and υ(C-O) appear at 1507 cm^{-1} (exp. 1418 cm^{-1}) and 1385 cm^{-1} (exp. 1319 cm^{-1}), respectively.

Although single crystals could not be isolated for these complexes, the analytical, spectroscopic, magnetic data and DFT calculation enable us to predict possible structures as shown in Figure 3.

Anticancerous and Antiproliferative Activity

Treatment of cell lines with increasing concentrations **A3** and its metal complexes resulted in variable degrees of inhibition. The highest activity was obtained for **CuA3** with IC_{50} values of 94.03 and 150.45 μM against MCF-7 and HCT 116 cell lines, respectively (Table 4). Additionally, this compound exhibited low toxicity against Vero normal cell line with IC_{50} value >320 μM. These results are close to those obtained with cisplatin (positive control) which inhibited both cancer cell lines at a concentration of around 58 μM and showed lower toxicity against Vero cell line (IC_{50} >416.6 μM).

The ligand showed activity against MCF-7 cell line (IC_{50} = 101.89 μM) and it was nontoxic against HCT 116 and Vero cells (IC_{50} >320 μM). On the other hand, Mn and Zn complexes showed lower activity compared with **CuA3** which has the lowest IC_{50} value (94.03 μM) against MCF-7 cell line (Table 4). These results indicate that adding Mn and Zn to the ligand may reduce its anticancer activity.

Compounds	MCF-7	HCT 116	VERO
A3	101.89 ±1.4	>320	>320
MnA3	278.80 ±2.2	>320	>320
ZnA3	167.61 ±0.1	>320	>320
CuA3	94.03 ±4.7	150.45 ±2.8	>320
Cisplatin	58.32 ±2.1	58.32 ±0.4	>416.6

Table 4. The IC_{50} values (μM) of the ligand and its three derivatives on three cell lines (MCF-7, HCT 116 and Vero). Data are presented using mean ±SE from three independent experiments. The IC_{50} values were calculated using nonlinear regression in Statistical Package for the Social Sciences version 18 (SPSS Inc. Chicago, IL, USA)

CONCLUSIONS

New symmetrical Schiff base tetracoordinate ligands and their Cu(II), Mn(II) and Zn(II) complexes have been prepared and characterized by different spectroscopic techniques and elemental analysis. The complexes were found to be neutral and paramagnetic except the zinc complexes which were found to be diamagnetic.

The optimized ground state geometries, IR and UV-Vis spectral data for the complexes were reported using DFT calculations at the B3LYP/6–31G(d) level of theory and the obtained results were in good agreement with the experimental data. The anticancerous and antiproliferative activity of the **A3** ligand and its metal complexes were evaluated. The highest activity was obtained for **CuA3** against MCF-7 and HCT 116 cell lines.

CONFILICT OF INTEREST

The Authors declare that there is no conflict of interest

LITERATURE CITED

1. Costes, J.P., Dahan, F., Fernandez, M.B.F., Garcia, M.I.F., Deibe, A.M.G. & Sanmartin, J. (1998). General synthesis of 'salicylaldehyde half-unit complexes': structural determination and use as synthon for the synthesis of dimetallic or trimetallic complexes and of 'self-assembling ligand complexes'. *Inorg. Chim. Acta.* 274(1), 73–81. DOI: 10.1016/S0020-1693(97)05991-4.

2. Dalia, S.F., Afsan, F., Hossain, M.S., Khan, M.N., Zakaria, C., Kudrat-E-Zahan, M. & Ali, M.H. (2018). A short review on chemistry of Schiff base metal complexes and their catalytic application. *Int. J. Chem. Stud.* 6(3), 2859–2866.

3. Kumar, S., Dhar, D.N. & Saxena, P.N. (2009). Applications of metal complexes of Schiff bases-A review. *J. Sci. Ind. Res. India.* 68(3), 181–187.

4. Nishinaga, A., Yamada, T., Fujisawa, H., Ishizaki, K., Ihara, H. & Matsuura, T. (1988) Catalysis of cobalt-Schiff base complexes in oxygenation of alkenes: on the mechanism of ketonization. *J. Mol. Catal.* 48, 249–264. DOI: 10.1016/0304-5102(88)85009-0.

5. Sabaa, M.W., Mohamed, R.R. & Oraby, E.H. (2009). Vanillin–Schiff's bases as organic thermal stabilizers and co-stabilizers for rigid poly(vinyl chloride). *Eur. Polym. J.* 45(11), 3072-3080. DOI: 10.1016/j.eurpolymj.2009.08.018.

6. Tunçel, M. & Serin, S. (2006). Synthesis and characterization of new azo-linked Schiff bases and their cobalt(II), copper(II) and nickel(II) complexes. *Transit. Met. Chem*. 31, 805–812. DOI: 10.1007/s11243-006-0074-5.

7. Pandeya, S.N., Sriram, D., Nath, G. & De Clercq, E. (1999). Synthesis, antibacterial, antifungal and anti-HIV evaluation of Schiff and Mannich bases of isatin derivatives with 3-amino-2-methylmercapto quinazolin-4(3H)-one. *Pharm. Acta. Helv.* 74(1), 11–17. DOI: 10.1016/s0031-6865(99)00010-2.

8. Kelley, J.L., Linn, J.A., Bankston, D.D., Burchall, C.J., Soroko, F.E. & Cooper, B.R. (1995). 8-Amino-3-benzyl-1,2,4-triazolo[4,3-a]pyrazines. Synthesis and anticonvulsant activity. *J. Med. Chem.* 38(18), 3676–3679. DOI: 10.1021/jm00018a029.

9. Pavan, F.R., Maia, P., Leite, S.R.A., Deflon, V.M., Batista, A.A., Sato, D.N., Franzblau, S.G. & Leite, C.Q.F. (2010). Thiosemicarbazones, semicarbazones, dithiocarbazates and

hydrazide/hydrazones: anti-mycobacterium tuberculosis activity and cytotoxicity. *Eur. J. Med. Chem.* 45(5), 1898–1905. DOI: 10.1016/j.ejmech.2010.01.028.

10. Upadhyay, K.K., Kumar, A., Upadhyay, S. & Mishra, P.C. (2008). Synthesis, characterization, structural optimization using density functional theory and superoxide ion scavenging activity of some Schiff bases. *J. Mol. Struct.* 873, 5–16. DOI: 10.1016/j.molstruc.2007.02.031.

11. Dutta, B., Some, S. & Ray, J.K. (2006). Thermal cyclization of 3-arylamino-3-(2-nitrophenyl)-propenal Schiff base hydrochlorides followed by triethyl phosphite mediated deoxygenation: a facile synthesis of quindolines. *Tetrahedron Lett.* 47(3), 377–379. DOI: 10.1016/j.tetlet.2005.11.007.

12. Chandramouli, Shivanand, M.R., Nayanbhai, T.B., Bheemachari & Udupi, R.H. (2012). Synthesis and biological screening of certain new triazole Schiff bases and their derivatives bearing substituted benzothiazole moiety. *J. Chem. Pharm. Res.* 4(2), 1151–1159.

13. Chinnasamy, R.P., Sundararajan, R. & Govindaraj, S. (2010). Synthesis, characterization, and analgesic activity of novel Schiff base of isatin derivatives. *J. Adv. Pharm. Tech. Res.* 1(3), 342–347. DOI: 10.4103/0110-5558.72428.

14. Chaubey, A.K. & Pandeya, S.N. (2012). Synthesis & anticonvulsant activity (chemo shock) of Schiff and Mannich bases of isatin derivatives with 2-amino pyridine (mechanism of action). *Int. J. Pharmtech Res.* 4(2), 590–598.

15. Aboul-Fadl, T., Mohammed, F.A. & Hassan, E.A. (2003). Synthesis, antitubercular activity and pharmacokinetic studies of some Schiff bases derived from 1-alkylisatin and isonicotinic acid hydrazide (INH). *Archiv. Pharm. Res.* 26(10), 778–784. DOI: 10.1007/BF02980020.

16. Miri, R., Razzaghi-asl, N. & Mohammadi, M.K. (2013). QM study and conformational analysis of an isatin Schiff base as a potential cytotoxic agent. *J. Mol. Mod.* 19(2), 727–735. DOI: 10.1007/s00894-012-1586-x.

17. Avaji, P.G., Kumar, C.H.V., Patil, S.A., Shivananda, K.N. & Nagaraju, C. (2009). Synthesis, spectral characterization, in-vitro microbiological evaluation and cytotoxic activities of novel macrocyclic bis hydrazine. *Eur. J. Med. Chem.* 44(9), 3552–3559. DOI: 10.1016/j.ejmech.2009.03.032.

18. Rao, S.N., Kathale, N., Rao, N.N. & Munshi, K.N. (2007). Catalytic air oxidation of olefins using molybdenum dioxo complexes with dissymmetric tridentate O,N,S-donor Schiff base ligands derived from o-hydroxyacetophenone and S-benzyldithiocarbazate or S-methyldithiocarbazate. *Inorg. Chim. Acta.* 360(14), 4010–4016. DOI: 10.1016/j.ica.2007.05.035.

19. Iwakura, I., Ikeno, T. & Yamada, T. (2004). Proposal for the metallacycle pathway during the cyclopropanation catalyzed by cobalt−Schiff base complexes. *Org. Lett.* 6(6), 949–952. DOI: 10.1021/ol036505m.

20. Nishinaga, A., Yamada, T., Fujisawa, H., Ishizaki, K., Ihara, H. & Matsuura, T. (1988). Catalysis of cobalt-Schiff base complexes in oxygenation of alkenes: on the mechanism of ketonization. *J. Mol. Catal.* 48, 249–264. DOI: 10.1016/0304-5102(88)85009-0.

21. Al-Shboul, T.M.A., Ziemann, S., Görls, H., Jazzazi, T.M.A., Krieck, S. & Westerhausen, M. (2018). Synthesis of dipotassium 2,2′-bis(2-oxidobenzylideneamino)-4,4′-dimethyl-1,1′-biphenyl derivatives and use as ligand transfer reagent. *Eur. J. Inorg. Chem.* 2018(14), 1563–1570. DOI: 10.1002/ejic.201701472.

22. Al-Shboul, T.M.A., Ziemann, S., Görls, H., Krieck, S. & Westerhausen, M. (2019). Substituted 2,2′-bis(2-oxidobenzylideneamino)-4,4′-dimethyl-1,1′-biphenyl complexes of zinc. *Z. Anorg. Allg. Chem.* 645(3), 292–300. DOI: 10.1002/zaac.201800404.

23. Jazzazi, T.M.A., Ababneh, T.S. & Abboushi, E.K. (2019). Zinc(II) complexes of symmetrical tetradentate Schiff base ligands derived from 2,2'-diamino-6,6'-dibromo-4,4'-dimethyl-1,1'-biphenyl-salicylaldehyde: synthesis, characterization and computational study. *Jordan J. Chem.*14(2), 81–87.

24. Carlin, R.B. & Foltz, G.E. (1956). Ullmann synthesis of six dimethyldinitrobiphenyls and their reduction to the corresponding diaminodimethylbiphenyls. *J. Am. Chem. Soc.* 78(9), 1997–2000. DOI: 10.1021/ja01590a065.

25. Spartan'18 Wavefunction. Inc. Irvine, CA.

26. Becke, A.D. (1993). Density-functional thermochemistry. III. The role of exact exchange. *J. Chem. Phys.* 98(7), 5648–5652. DOI: 10.1063/1.464913.

27. Becke, A.D. (1996). Density-functional thermochemistry. IV. A new dynamical correlation functional and implications for exact-exchange mixing. *J. Chem. Phys.* 104(3), 1040–1046. DOI: 10.1063/1.470829.

28. Lee, C., Yang, W. & Parr, RG. (1988). Development of the Colle-Salvetti correlation-energy formula into a functional of the electron density. *Phys. Rev. B.* 37(2), 785–789. DOI: 10.1103/PhysRevB.37.785.

29. Petersson, G.A., Bennett, A., Tensfeldt, T.G., Al-Laham, M.A & Shirley, W.A. (1988). A complete basis set model chemistry. I. The total energies of closed-shell atoms and hydrides of the first-row elements. *J. Chem. Phys.* 89(4), 2193–2218. DOI: 10.1063/1.455064.

30. Petersson, G.A., Tensfeldt, T.G. & Montgomery, J.A. (1991). A complete basis set model chemistry. III. The complete basis setquadratic configuration interaction family of methods. *J. Chem. Phys.* 94(9), 6091–6101. DOI: 10.1063/1.460448.

31. Talib, W.H. (2017). Regressions of breast carcinoma syngraft following treatment with piperine in combination with thymoquinone. *Sci. Pharm.* 85(3), 27. DOI: 10.3390/scipharm85030027.

32. Jayaseelan, P., Prasad, S., Vedanayaki, S. & Rajavel, R. (2016). Synthesis, characterization, anti-microbial, DNA binding and cleavage studies of Schiff base metal complexes. *Arab. J. Chem*. 9, 668–677. DOI: 10.1016/j.arabjc.2011.07.029.

33. Yousif, E., Majeed, A., Al-Sammarrae, K., Salih, N., Salimon, J. & Abdullah, B. (2017). Metal complexes of Schiff base: Preparation, characterization and antibacterial activity. *Arab. J. Chem*. 10, 1639–1644. DOI: 10.1016/j.arabjc.2013.06.006.

34. Thaker, B.T., Surati, K.R., Oswal, S., Jadeja, R.N. & Gupta, V.K. (2007). Synthesis, spectral, thermal and crystallographic investigations on oxovanadium(IV) and manganese(III) complexes derived from heterocyclic β-diketone and 2-amino ethanol. *Struct. Chem.* 18, 295–310. DOI: 10.1007/s11224-006-9134-x.

35. Miessler, G. & Tarr, D. (2005). *Inorganic Chemistry* (3rd ed). New Jersey, USA: Pearson Prentice-Hall.

36. Ababneh, T.S., Al-Shboul, T.M.A., Jazzazi, T.M.A., Alomari, M.I., Görls, H. & Westerhausen, M. (2020). Crystallographic and computational study of the structure of copper(II) 2,2′-bis(2-oxidobenzylideneamino)-4,4′-dimethyl-1,1′-biphenyl. *Transit. Met. Chem*. 45. DOI: 10.1007/s11243-020-00395-8

37. Cheeseman, T.P., Hall, D. & Waters, T.N. (1966). The colour isomerism and structure of some copper co-ordination compounds. Part XII. The crystal structure of NN′-(2,2′-biphenyl)bis(salicylaldiminato)copper(II). *J. Chem. Soc. A* 1396–1406. DOI: 10.1039/J19660001396.

38. Taha, Z.A., Ajlouni, A.M., Ababneh, T.S., Al-Momani, W., Hijazi, A.K., Al Masri, M. & Hammad, H. (2017). DFT computational studies, biological and antioxidant activities, and kinetic of thermal decomposition of 1,10-phenanthroline lanthanide complexes. *Struct. Chem.* 28, 1907–1918. DOI: 10.1007/s11224-017-0975-2.